Radial and latitudinal dependencies of discontinuities in the solar wind between 0.3 and 19 AU and ?80° and +10°

A. Söding, F. M. Neubauer, B. T. Tsurutani, N. F. Ness, R. P. Lepping

Annales Geophysicae (2001) 19: 667–680 © European Geophysical Society 2001

Annales Geophysicae

Radial and latitudinal dependencies of discontinuities in the solar wind between 0.3 and 19 AU and $-80°$ and $+10°$

A. Söding[1], **F. M. Neubauer**[1], **B. T. Tsurutani**[2], **N. F. Ness**[3], **and R. P. Lepping**[4]

[1]Institut für Geophysik und Meteorologie, Universität zu Köln, Köln, Germany
[2]Jet Propulsion Laboratory, California Institute of Technology, Pasadena, USA
[3]Bartol Research Foundation, University of Delaware, Newark, USA
[4]Laboratory for Extraterrestrial Physics, Greenbelt, Goddard Space Flight Center, USA

Received: 17 January 2000 – Revised: 28 February 2001 – Accepted: 11 April 2001

Abstract. Directional discontinuities (DD) from 5 missions at 7 different locations between 0.3 and 19 AU and $-80°$ and $+10°$ in the 3D heliosphere are investigated during minimum solar activity. The data are surveyed using the identification criteria of Burlaga (1969) (B) and Tsurutani and Smith (1979) (TS). The rate of occurrence depends linearly on the solar wind velocity caused by the geometric effect of investigating a larger plasma volume if the solar wind velocity v_{sw} increases. The radial dependence is proportional to $r^{-0.78}$ (TS criterion) and $r^{-1.28}$ (B criterion), respectively. This dependence is not only due to an increasing miss rate with increasing distance. The DDs must be unstable or some other physical effect must exist. After normalization of the daily rates to 400 km/s and 1 AU, no dependence on heliographic latitude or on solar wind structures is observable. This means that the DDs are uniformly distributed on a spherical shell. Normalized 64 DD per day are identified with both criteria. But large variations of the daily rate still occur, indicating that other influences must exist. The ratio of the rates of rotational (RDs) and tangential discontinuities (TDs) depends on the solar wind structures. In high speed streams, relatively more RDs exist than in low speed streams. In the inner heliosphere ($r < 10$ AU), no radial or latitudinal dependence of the portions of the DD types occur. 55% clear RDs, 10% clear TDs and 33% EDs (either discontinuities) are observed, but the portions differ with regard to the criteria used. In the middle heliosphere (10 AU $< r <$ 40 AU), the DD types are more uniformly distributed. The distribution of the directional change ω over the transition evolves to an increase of smaller ω with increasing distance from the sun. The evolution is yielded by the anisotropic RDs with small ω. The spatial thickness d_{km} in kilometers increases with distance. The thickness d_{rg} normalized to the proton gyro radius decreases by a factor of 50 between 0.3 and 19 AU, from $201.3\,r_g$ down to $4.3\,r_g$. In the middle heliosphere, the orientation of the normals relative to the local magnetic field is essentially uniform except for the parallel direction where no DDs occur. This indicates that RDs propagating parallel to $\boldsymbol{B}$ play a special role. In addition, in only a few cases is $[\boldsymbol{v}]$ parallel to $[\boldsymbol{B}/\rho]$, which is required by the MHD theory for RDs. The DDs have strongly enhanced values of proton gyro radius r_g for $\omega \sim 90°$. In contrast, in the inner heliosphere, only a small increase in r_g with ω is observed.

Key words. Interplanetary physics (discontinuities; interplanetary magnetic fields) – Space plasma physics (discontinuities)

1 Introduction

Discontinuities are fundamental features in the interplanetary medium on the microscale (Burlaga, 1969). They provide indications of the internal structure of the solar wind and its evolution. Most of the discontinuities are generated at or near the Sun (Tsurutani and Smith, 1979), but also a local generation is possible (Ho et al., 1995, 1996).

The goal of our paper is to investigate, statistically, discontinuities at different positions in the three-dimensional (3D) heliosphere to obtain a global overview of their properties. Radial and latitudinal dependences, as well as dependences on solar wind structures, are determined to obtain information on the evolution and generation of the discontinuities. Such investigations have been carried out previously by several authors and also for different positions in the heliosphere (e.g. Burlaga, 1969; Tsurutani and Smith, 1979; Neugebauer et al., 1984; Lepping and Behannon, 1986). But since they all used (partly) different identification criteria and intervals with different solar activity states, the results are only comparable in a limited way. We use the same criteria for all intervals which take place during solar activity minimum. In this study, we distinguish between the different types of discontinuities: rotational (RD), tangential (TD) and either (ED) (Neugebauer et al., 1984).

First, the missions, data and intervals used are described to show which locations in the 3D heliosphere are covered.

Correspondence to: A. Söding (soeding@geo.uni-koeln.de)

Table 1. Missions, times, heliographic latitude θ and distance r from the Sun of the 7 intervals

Mission	Interval	θ [deg]	r [AU]
Voyager 2	7/11/1985 – 25/02/1986	0.	19.0
Ulysses I	1/09/1994 – 27/09/1994	−80.22	2.3
II	10/01/1995 – 5/02/1995	−30.	1.5
III	19/02/1995 – 17/03/1995	0.	1.3
Wind	5/04/1995 – 1/05/1995	0.	1.0
IMP 8	5/04/1995 – 1/05/1995	0.	1.0
Helios 2	2/04/1976 – 28/04/1976	0.	0.3

Table 2. Number of identified DDs in the intervals, the number of the ones used and the number of the usable transitions

Mission	identified	used	%	N_0
Voyager 2	1430	1430	100	924
Ulysses I	2514	1360	54	1435
II	2631	1360	52	1381
III	1397	1397	100	1469
Wind	1682	1682	100	1651
IMP 8	720	720	100	690
Helios 2	2162	1510	70	1591
All	12536	9459	75	9141

Briefly, the identification criteria of the discontinuities and the detailed numbers of the discontinuities are presented. The discontinuities are investigated with respect to the properties, such as the rate of occurrence, the directional change over the transition, the distribution of the types of discontinuities, the thickness and the differences between the inner and the middle heliosphere. The paper is brought to a close by a summary of the observations and their discussion.

2 Missions, data, intervals, and identification criteria

Data from seven intervals with different distances and latitudes from five different vehicles are used. For Ulysses, three intervals from different heliographic latitudes are chosen: high ($\sim -80°$, 2.3 AU), mid ($\sim -30°$, 1.5 AU) and low ($\sim 0°$, 1.3 AU) latitudes. At 1 AU, we use the same time interval for Wind and IMP 8 to estimate differences due to different satellites. With Helios 2, a position is given at 0.3 AU and with Voyager 2, at 19 AU. Therefore, we cover a wide range of heliospheric distances and latitudes. Each interval has the duration of 27 days except for Voyager 2, which contains 84 days in order to find enough discontinuities for the statistical investigations. Since the measurements of the missions were not available at the same times, we chose similar solar wind states, i.e. during the minimum of solar activity. The missions, times, distances r from the Sun and latitudes θ used are summarized in Table 1.

For the analysis, we used the data from the magnetometer and the plasma experiments of each spacecraft. For a description of the instruments, we refer to the following papers: Lepping et al. (1995), Ogilvie et al. (1995), Musmann et al. (1977), Rosenbauer et al. (1977), Behannon et al. (1977), Hartle et al. (1982), Balogh et al. (1992) and Bame et al. (1992). The minimum sampling period ranges between 0.25 s for Helios 2, and 3 s for Wind. Ulysses has a sampling period of 1 or 2 s, IMP 8 of 1.28 s and Voyager 2 of 1.92 s.

For the identification of directional discontinuities (DD), we use the criteria of Burlaga (1969) (B) and Tsurutani and Smith (1979) (TS). The former has, as the main condition, a change in the direction of the magnetic field $\boldsymbol{B}$ of more than 30° during 60 s and the latter requires $|\Delta \boldsymbol{B}|/B_{\max} \geq 0.5$ with $\Delta \boldsymbol{B} = \boldsymbol{B}_i - \boldsymbol{B}_{i-k}$ and $k = 3$ using 60 s averages. The main condition of the TS criterion is more general than that of the B criterion since not only changes in the direction are considered, but also changes in the magnitude. This means that due to the main conditions, all DDs identified by B are included in the subset of DDs identified by TS. But due to additional conditions, in a few cases, it is also possible that a DD is only identified by the B criterion. In our analysis, it is only necessary that a DD fulfills at least one of the criteria.

More than 12,000 DDs are identified (Table 2) and from these, 9459 DDs are visually inspected in the highest available sampling rate. If there are no data gaps inside or around the transition and no artificial oscillations, the beginning and the end are marked.

An example of a discontinuity with the marked beginning and end of the chosen current sheet is given in Fig. 1, with the magnitude and the polar angles ϕ and θ of the high resolution magnetic field in RTN coordinates. In this frame of reference, the Sun is in the center and R points radial from the Sun to the satellite. T is perpendicular to R, and parallel to the solar equator, and points in the direction of the orbital motion. N completes the system.

When there are 4 or more data points inside the transition, an additional minimum variance analysis (MVA) based on Sonnerup and Cahill (1967) is calculated. Otherwise, the possible DD is rejected. N_0 is the resulting number of DDs which could be used for the statistical investigations. In our case, these are 9141 DDs.

3 Rate of occurrence

The rate of occurrence of DDs (DD per day) is investigated with regard to the dependences of solar wind structures, radial distances r, solar wind velocities v and heliographic latitudes θ. The quantity DD per day is corrected with respect to data gaps. For Helios 2, an additional correction is necessary because the azimuthal speed of the spacecraft φ_H is in the same order as the angular velocity φ_{sun} of the Sun (Barnstorf, 1980). The multiplicative factor used is $z = 1/(1 - \varphi_H/\varphi_{\text{sun}})$. At the perihel, z increases up to 2.5.

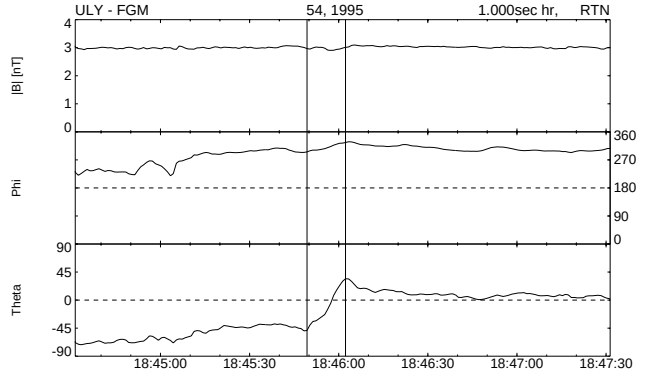

Fig. 1. Example of a discontinuity to show the choice of the beginning and the end of the layer.

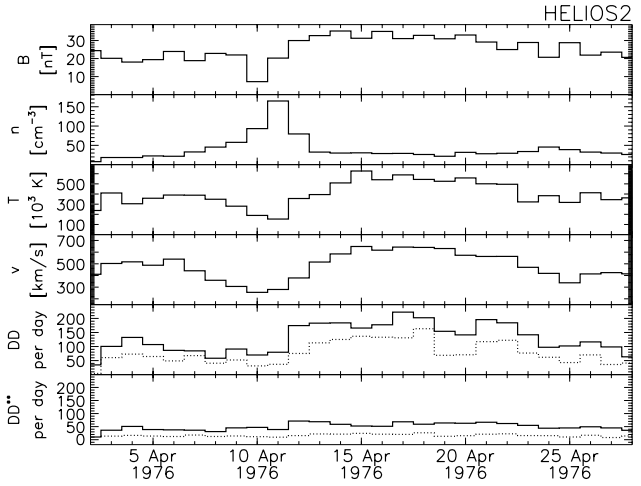

Fig. 2. Daily averages of B, n, T, v and the rates DD per day and DD** per day for the TS (solid) and B (dashed) criteria, respectively.

3.1 Dependence on solar wind structures

The variations in the rates of DD per day and of plasma parameters are shown, for example, in Fig. 2, in the case of the Helios 2 interval. The daily averages are shown (top to bottom) of the magnetic field B, the density n, the temperature T, the solar wind velocity v and the rates of the DD per day and DD** per day (DD per day normalized to 400 km/s and 1 AU) for the TS (solid) and B (dotted) criteria, respectively. The last panel will be discussed later. The corotating interaction regions are clearly visible. The rates of DD per day are obviously correlated with the solar wind velocity and the temperature for both criteria. The faster the solar wind is, the higher the rates are. This has previously been observed by Burlaga et al. (1977), Solodyna et al. (1977), Barnstorf (1980) and Lepping and Behannon (1986).

Approximately twice as many DDs are identified when comparing the TS criterion to the B criterion. In all intervals, a large variation from day-to-day occurs up to a factor of 8, which has also been seen by several other authors (e.g. Burlaga et al., 1977; Barnstorf, 1980; Lepping and Behannon, 1986; Tsurutani et al., 1994; Ho et al., 1996). Tsurutani and Smith (1979) also observed a variation from one solar rotation to the next solar rotation by a factor of 2.5.

One could conclude that the rate of occurrence of DDs seems depend on the large scale structure of the solar wind. But not all variations could be explained by these dependences.

3.2 Radial dependence

To investigate the radial dependence of the rate of occurrence, the distribution of DD per day over the logarithm of the radial distance r with a bin size of 0.1 AU is calculated (Fig. 3). Additionally, the standard deviations are shown with error bars. A strong decrease with increasing distance is observable and this confirms the former results (e.g. Burlaga, 1971b; Mariani et al., 1973). The least square root fit to the rates measured in the ecliptic plane (dark) is given in the figure. Therefore, the measurements are weighted by the inverse of the standard deviation. The measurements out of the ecliptic (lighter) do not fit the distribution. This could be due to the higher latitude and therefore, to higher solar wind velocities. This will be investigated in the following section.

For the rates measured in the ecliptic plane, the radial decrease is proportional to $r^{-0.78}$ and $r^{-1.28}$ for the TS criterion and the B criterion, respectively. Particularly for the B criterion, Lepping and Behannon (1986) observed in Mariner 10 data the same dependence. The fits for a function proportional to $\exp(-r/r_s)$ (Tsurutani and Smith, 1979; Tsurutani et al., 1996) are worse.

3.3 Dependence on solar wind velocity

One might expect a correlation of the rates with the solar wind velocity, since under the assumption of uniformly distributed DDs which only convect with the solar wind, the larger v is, the larger the rate of DDs is. This is a geometric effect due to a larger investigated plasma volume during the same time.

The fact that a correlation exists is shown in Sect. 3.1 and confirmed in Fig. 4, where the rates of DD per day versus v are displayed. For each daily rate, a "+" sign is drawn. The linear increase of DD per day with v is clarified by the overlying linear regression (solid line). The resulting functions are $(-15.8 \pm 10.7) + (0.166 \pm 0.018) \cdot v$ for the TS criterion and $(-15.6 \pm 7.6) + (0.098 \pm 0.013) \cdot v$ for the B criterion. Within the errors, the relationship is also consistent with a linear dependence through the origin, as suggested in the first paragraph. Qualitatively, this is also seen from Barnstorf (1980) and Tsurutani et al. (1994). However, large fluctuations of the daily rates exist and could not be explained only by the large scale solar wind structure.

Due to the normalization of the rates to 400 km/s ($\rightarrow$ DD* per day), most of the dependence on the velocity is removed from the data, if the solar wind velocities and the rates are very low (small negative rates could occur due to the normal-

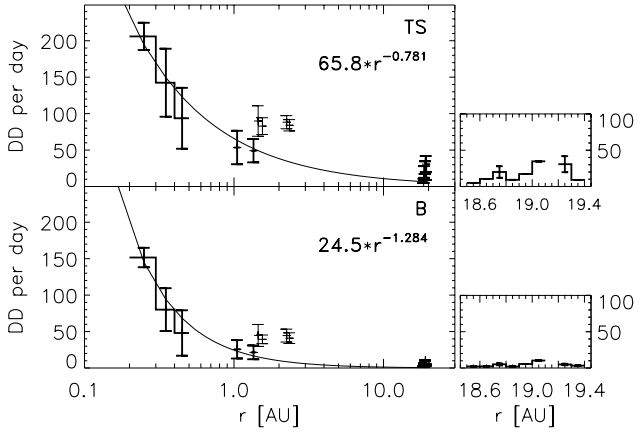

Fig. 3. Distribution of DD per day over r with a bin size of 0.1 AU and the standard deviations as error bars on logarithmic scale; TS criterion at the top and B at the bottom; darker lines represent intervals in the ecliptic which are used for the given fit and lighter ones are out of the ecliptic; right Voyager 2 in detail on linear scale.

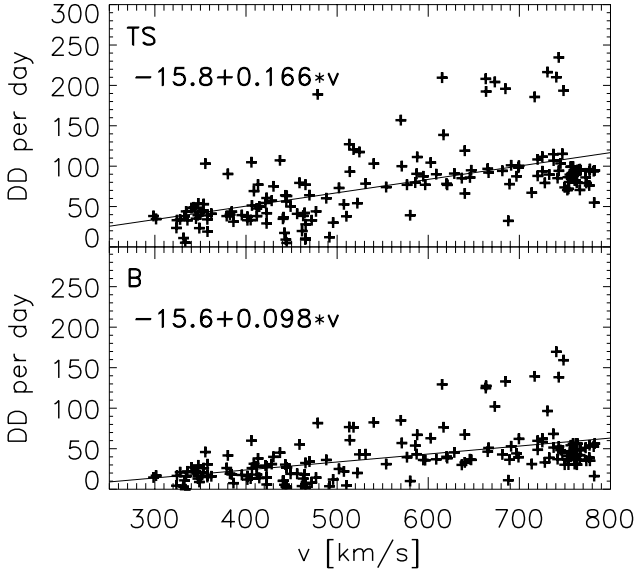

Fig. 4. Distribution of daily averages of DD per day over v (top: TS, bottom: B criterion) with the fit of an linear function.

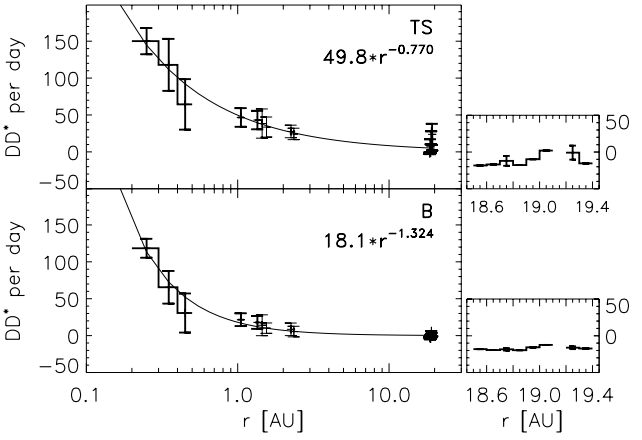

Fig. 5. Distribution of DD* per day normalized on 400 km/s over r with a bin size of 0.1 AU; analog to Fig. 3.

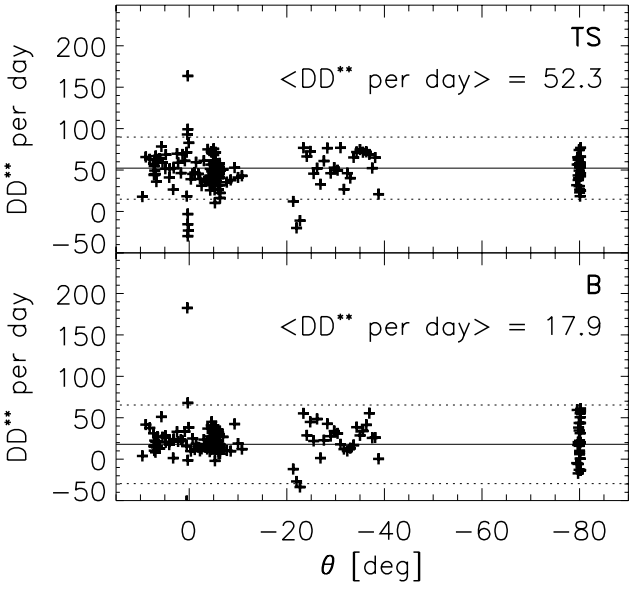

Fig. 6. Distribution of DD** per day normalized on 400 km/s and 1 AU versus θ; average (solid) and standard deviation (dotted) are shown.

ization). This happens partly for the Voyager 2 rates. Similar to the DD rates shown in Fig. 3, the radial dependence of the DD* rates per day, is displayed in Fig. 5. In contrast to the rate of DD per day , the DD* per day from intervals out of the ecliptic now agrees very well with the distribution in the ecliptic. From the comparison of the exponents given in Figs. 3 and 5, it is obvious that the dependences on the velocity and radial distance are independent from each other.

3.4 Dependence on heliographic latitude

To test the dependence on the heliographic latitude θ, the rates are normalized to 400 km/s and 1 AU ($\rightarrow$ DD** per day), which is displayed in Fig. 6 for each daily rate versus θ. We cover the range between +10° and −80°. Large fluctuations are again observable, but there is no general trend. The mean (solid) and the standard deviations (dotted) are given. At 1 AU and with $v = 400$ km/s, on average, 52.3 DD per day (2.1 DDs/h) for the TS, and 17.9 DD per day (0.7 DDs/h) for the B criterion are observed. On the basis of Pioneer 10 and 11 data between only the ±6° heliographic latitude, this independence has been previously seen (Tsurutani and Smith, 1979).

The fact that the latitudinal dependence is caused only by the velocity dependence is elucidated in Fig. 7. The distribution of the rates DD$^\diamond$ per day normalized to 1 AU with a bin size of 5° versus θ and their standard deviation as error bars are shown. Additionally, the mean solar wind velocity of the events in each bin is marked by a "$\diamond$" sign. The scale of the

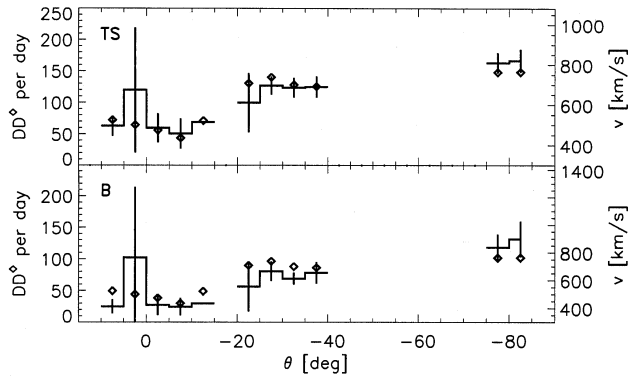

Fig. 7. Distribution of DD$^{\diamond}$ per day normalized on 1 AU with a bin size of 5° and average v ($\diamond$) over θ; top: TS, bottom; B criterion.

Table 3. Criteria to determine the types of the DDs (after Neugebauer et al., 1984)

DD type	$[B]/B_{\max}$	$B_n/B_{\max}$
TD	≥ 0.2	< 0.4
RD	< 0.2	≥ 0.4
ED	< 0.2	< 0.4
ND	≥ 0.2	≥ 0.4

velocity axis is chosen to agree well with the DD$^{\diamond}$ per day within the framework of their standard deviations. The rates of DD$^{\diamond}$ per day and v are correlated.

Now we will again examine the dependence on solar wind structures. In the lowest panel of Fig. 2, the rate DD** per day normalized to 1 AU and 400 km/s is displayed for both criteria. After the normalization, the large variations in the rates disappear. But there are still some smaller variations. It should be pointed out that after the normalization, no dependence of the rates of these microscale structures on the large-scale solar wind structures exists.

4 Distribution of DD types

In MHD theory, different types of discontinuities exist. Most of the DDs in the solar wind are RDs or TDs (Smith (1973); Belcher and Solodyna (1975); Solodyna et al., 1977). To distinguish between them, characteristic properties are used. We use the behavior of the normal component B_n and the change in the magnitude $[B]$ over the transition. The limits are given in Table 3 (after Neugebauer et al., 1984) with $B_{\max}$ as the larger value of B, before and after the transition. With these conditions clear RDs and clear TDs are defined, as well as two additional DD types, Either- (ED) and Neither- (ND) discontinuities, which are discussed later. To determine B_n, the direction of the normal $\boldsymbol{n}$ must be determined. Therefore, we employed the MVA. The uncertainty of $\boldsymbol{n}$ could be estimated by the ratio λ_2/λ_3 of the intermediate to the lowest

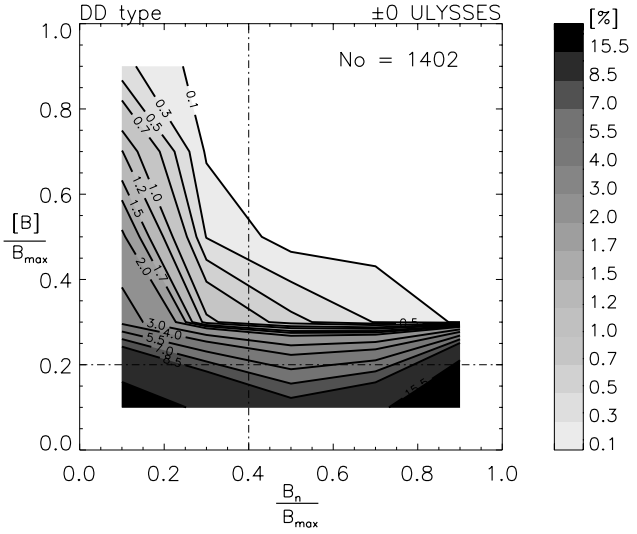

Fig. 8. Distribution of the DD phase space, for example, for the Ulysses III interval; dashed-dotted are the limits of the types; see text.

eigenvalue resulting from the MVA. A minimum ratio λ_2/λ_3 of 1.5 is imposed.

NDs have large B_n and large $[B]$, which is inconsistent with the MHD theory for RDs and TDs. On average, the ratio λ_2/λ_3 is smaller for NDs than for the other types. Hence, the determination of B_n is worse. Therefore, some of the NDs may be distorted TDs, and consequently, the number of clear TDs is only the lower limit of the existing TDs in the solar wind.

EDs have a small B_n and a small change in $[B]$. These properties apply to both RDs and TDs. Therefore, additional properties are necessary to assign an ED to a RD or TD. In Fig. 8, isolines of the relative frequency of DDs over the DD phase space (versus $B_n/B_{\max}$ and $[B]/B_{\max}$) are shown, for example, for Ulysses III. The isolines are shaded underneath and the bin size used is 0.2×0.2. The upper left corner represents TDs, the lower right RDs, the lower left EDs and the upper right NDs. For all missions, only DDs in the lower left triangle of the distibution occur. At small $[B]$, two peaks in the distribution exist: one with a large B_n and one with a small B_n. The former occurs due to the isotropic Alfvénic structures which propagate nearly parallel to the ambient magnetic field. The latter could, theoretically, occur due to degenerated RDs with a propagation direction nearly perpendicular to $\boldsymbol{B}$, or due to TDs with a constant B over the transition. Due to the increase of the DD phase space density for small B_n along the decreasing $[B]/B_{\max}$, and due to the decrease of the DD phase space density followed by an increase for small $[B]$ along B_n, we assume that most of the EDs are TDs. Again, the number of clear TDs is only the lower limit of the existing TDs in the solar wind.

In Fig. 9, the portions of the 4 DD types are shown for all intervals. Except for Voyager 2 and Helios 2 all distributions are similar. They have around 50–60 % RDs, up to 13 % TDs,

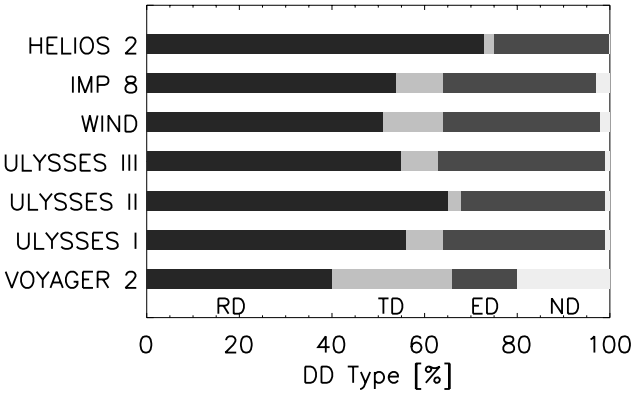

Fig. 9. Distribution of the DD types for the 7 intervals

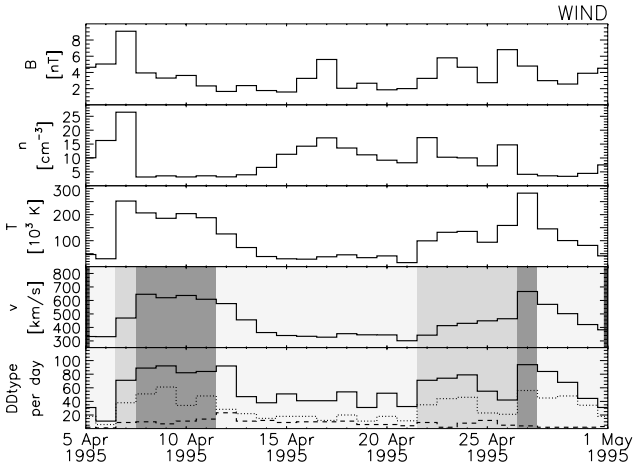

Fig. 10. Daily averages of B, n, T, v and the rates DD per day for overall DD (solid), RDs (dotted) and TDs (dashed), for example, for Wind for the TS and B criteria, respectively; shaded regions represent different solar wind states: peak region of v (dark), trailing edge (light), leading edge (intermediate).

25–35 % EDs and 2 % NDs. In case of Helios 2, some additional RDs and fewer TDs are identified compared to the other intervals. Contrary to our findings, Barnstorf (1980) identifies many more TDs in Helios 1 and 2 data. Therefore the portion of TDs may depend on the chosen interval. For Voyager 2, the types occur more uniformly. The portions of TDs (26 %) and of NDs (20 %) are clearly larger compared to the other intervals. The comparison of the three Ulysses intervals indicates that obviously no dependence on the heliographic latitude exist. Inside 2.3 AU, no radial dependence is observable. If one assumes that all EDs and NDs are, in reality, TDs, only a few more RDs than TDs are observed.

Our results are consistent with those of other authors (Lepping and Behannon, 1986; Smith, 1973; Tsurutani et al., 1996). If one determines the portions with respect to the identification criterion (B or TS) used, they differ except for Voyager 2. With only the TS criterion, a larger portion of RDs and a smaller one of TDs (-5 to -10 %) are identified. The lowest portion of RDs is found if the DDs are simultanously identified by both criteria. Neugebauer et al. (1984) investigated two intervals following each other where the portions differ by around 5 %. This indicates that there exists a wide range of variations in the portions.

4.1 Dependence on solar wind structures

In Sect. 3, it is shown that the rates of DDs depend on the large-scale solar wind structures, if they are not normalized to 400 km/s. In this section, we will focus on the rates of the different types of the DDs. Therefore, in Fig. 10, the daily averages of B, n, v and T (analogous to Fig. 2) and the overall rate of DDs (solid), as well as the rate of RD per day (dotted) and TD per day (dashed), are shown, for example, for the Wind interval. In the two lower panels, the different parts of the corotating interaction regions are marked by different shades; dark shading represents the peak regions of v, intermediate shading is the leading edge, and light shading is the trailing edge and the slow solar wind.

Qualitatively, in the peak region, the rates of DD per day and RD per day are high and low for TD per day. In the leading and trailing edges, fewer DDs are observed due to the lower v, but there is a tendency for more DDs and TDs to occur in the leading than in the trailing edges. Compared to the variations in the rate of RD per day , the rate of TD per day is nearly constant. The number of RD per day shows the same dependence as the overall DDs. Since no normalization is used in this figure, only the ratio of the rates of RDs and TDs should be considered. Due to the contrary variations of the RDs and TDs, the variation of the ratio will be increased by the normalization. The ratio RD/TD is much lower in the trailing edge than in the peak region and the leading edge. This means a dependence on the solar wind structures exists for the ratio RD/TD. In regions with a higher solar wind velocity, more RDs are observable.

The rate of the ED per day is nearly independent of the solar wind structures. Similar to the rate of TDs, no clear correlation with v is observable for EDs. This is an indication that they are primarily not RDs, but TDs. In the trailing edge, the same rates of ED per day and RD per day occur.

5 Directional change of the magnetic field

We investigated the directional change ω of the magnetic field across the interface. ω is defined as $\arccos[(\boldsymbol{B}_1 \cdot \boldsymbol{B}_2)/(|\boldsymbol{B}_1| \cdot |\boldsymbol{B}_2|)]$ between the first ($\boldsymbol{B}_1$) and the last ($\boldsymbol{B}_2$) vector of the transition. Discontinuities with $\omega < 30°$ could exist because the detailed analysis is based on higher time resolution data than that used in the identification according to the B and TS criteria.

For example the histograms of ω with a bin size of 15° for the Helios 2 (top) and Voyager 2 (bottom) intervals are presented in Fig. 11. A strong decrease for $\omega > 30°$ occurs. The comparison of the distributions shows that far away, relatively more DDs with $\omega < 45°$ exist than closer to the Sun. The mean and median are displayed in the figures.

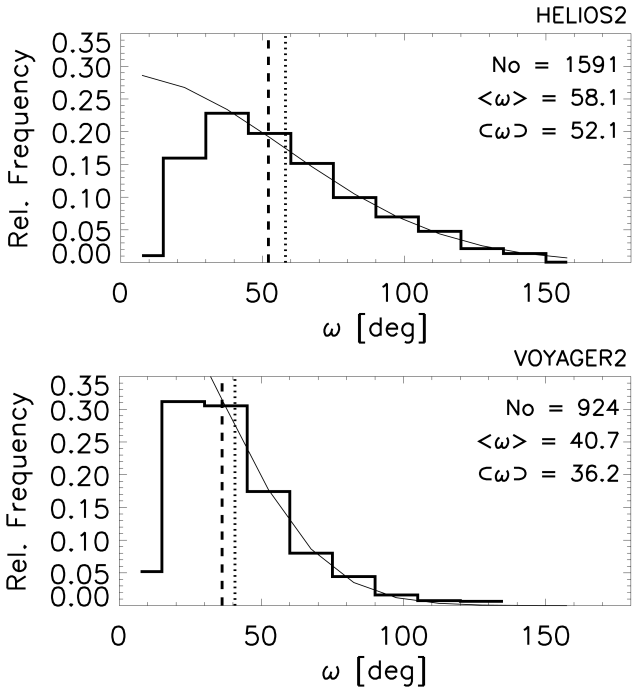

Fig. 11. Relative frequency of ω for Helios 2 (top) and Voyager 2 (bottom) as a histogram; thin solid line is a fit to the distribution proportional to $\exp[-(\omega/\omega_s)^2]$; the mean $\langle\omega\rangle$ is dotted and the median $\subset\omega\supset$ dashed shown.

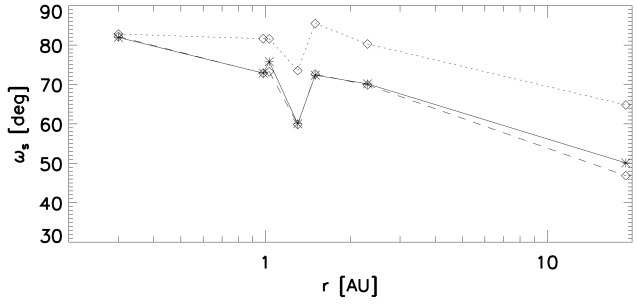

Fig. 12. Radial dependence of the fit parameter ω_s for the overall distribution (solid), the B criterion (dotted) and the TS (dashed).

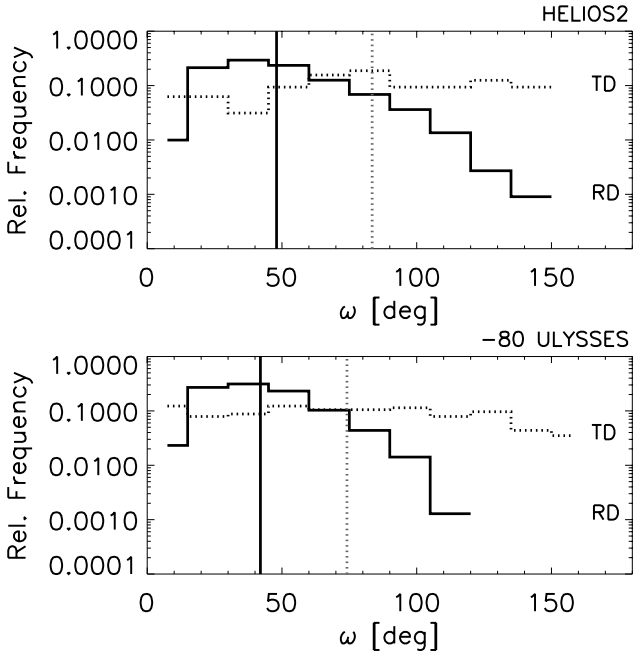

Fig. 13. Relative frequency of ω for Helios 2 (top) and Ulysses I (bottom) for RDs (solid) and TDs (dotted); the mean is given by the vertical lines.

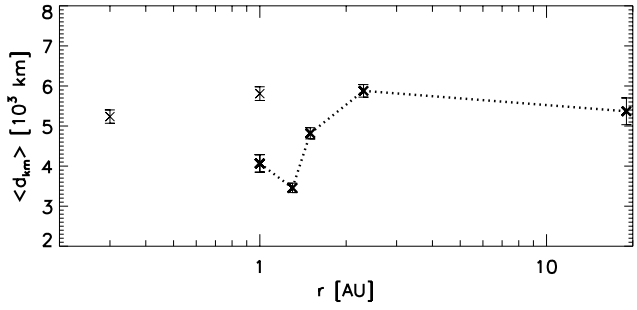

Fig. 14. Radial dependences of the mean thickness $\langle d_{\rm km}\rangle$ for the overall distribution; the mean error is shown by error bars.

The part of the distribution with $\omega \geq 30°$ is used to fit it to a function proportional to $\exp[-(\omega/\omega_s)^2]$ (thin line), where ω_s scales the decrease. The radial variation of ω_s is displayed in Fig. 12 (solid). A decrease with increasing r occurs. This form of the distribution has been previously observed (Burlaga, 1971a; Mariani et al., 1973; Barnstorf, 1980). In Pioneer 6 data at 1 AU, Burlaga (1969, 1971b) determines ω_s to be 75°, which is in good agreement with our results for Wind and IMP 8.

The radial dependence on ω_s differs (Fig. 12) for DDs identified by the TS or B criteria. For the B criterion (dotted) inside 2.3 AU, no radial dependence exists. But for the TS criterion (dashed), a radial dependence is observed which is very similar to the overall distribution.

The distribution of ω also depends on the different DD types: in Fig. 13, for example, for Helios 2 and Ulysses I, the histograms of ω for RDs (solid) and TDs (dotted) are shown, and the distributions differ for these types. The relative frequency of RDs decreases with increasing ω for $\omega > 30°$, and with increasing r, fewer RDs with large ω are observed. TDs are distributed more uniformly, and the most probable, ω is between 75° and 90°. Except for the Voyager 2 cases, on average, the directional change of the RDs is much smaller than for the TDs and EDs (vertical lines). The EDs have a similar distribution to the TDs. For Voyager 2, the DD types have the same distributions comparable with those of RDs closer to the Sun.

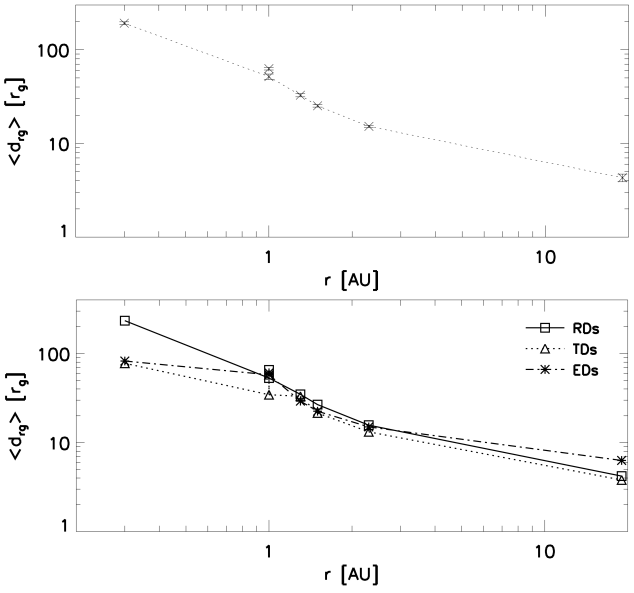

Fig. 15. Radial dependences of the mean thickness $\langle d_{rg} \rangle$ normalized to the proton gyro radius r_g for the overall distribution (top) and the DD types (bottom).

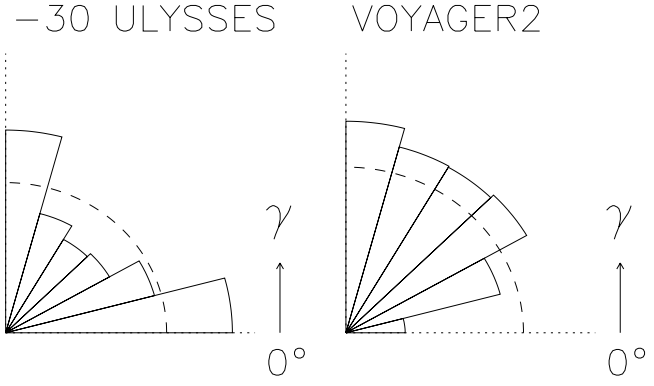

Fig. 16. Distribution of the angle γ between $\boldsymbol{n}$ and the mean magnetic field in the layer for Ulysses II (for the inner heliosphere) and Voyager 2 (middle heliosphere); the dashed circle indicates a uniform distribution.

6 Thickness of DDs

The thickness $d_{\rm km}$ of a discontinuity is determined by $d_{\rm km} = (\boldsymbol{v} \cdot \boldsymbol{n})\, \Delta T_t$ with $\boldsymbol{v} = \boldsymbol{v}_{sw} - \boldsymbol{v}_{s/c} + \boldsymbol{U}$, ΔT_t the transition time, $\boldsymbol{v}_{sw}$ the solar wind velocity, $\boldsymbol{v}_{s/c}$ the velocity of the spacecraft and $\boldsymbol{U}$ the propagation speed of the discontinuities. Only for Helios 2 is $\boldsymbol{v}_{s/c}$ not negligible.

The transition time ΔT_t is determined in highest resolution data. The mean value of the penetration time varies between 11 and 25 s for the different intervals. For example, the difference of the means $\langle \Delta T_t \rangle$ for Wind and IMP 8 (same time interval) is around 5 s. The reason for this is the different time resolutions of 3 s for Wind and 1.28 s for IMP 8; therefore, a systematic error is produced. We must restrict the analysis to include only missions with a sampling period between 1 and 2 s for the proper interpretation of $d_{\rm km}$. This means the results of Helios 2 and Wind should be excluded.

In Fig. 14, the radial dependence of the mean thickness $\langle d_{\rm km} \rangle$ is shown for all missions. The results for Wind and Helios 2 are not connected with the other ones because the sampling periods differ greatly. As expected from former investigations (Barnstorf, 1980; Lepping and Behannon, 1986), between 1 and 2.3 AU, an increase of $\langle d_{\rm km} \rangle$ is observed. Regardless of DD type, the same dependency is seen.

The systematic error is significant, especially for thin DDs. If one restricts the investigation to thick DDs ($\Delta T_t > 15$ s), for all missions between 0.3 and 2.3 AU, an increase of $\langle d_{\rm km} \rangle$ occurs with distance.

Due to the short penetration times, it is necessary to examine these phenomena on a kinetic scale. Therefore, we normalize the thickness of the proton gyro radius r_g, which is a characteristic length scale of the local plasma. Due to the large increase in r_g with r, the systematic errors are negligible. In Fig. 15, the radial dependence of $\langle d_{rg} \rangle$ of all DDs (top), as well as for the different DD types (bottom) is shown. Over the whole radial range, a strong decrease is observable and in this process, the thickness $\langle d_{rg} \rangle$ is reduced by a factor of 50 from $201.3\, r_g$ to $4.3\, r_g$. Except for the large difference in the DD types for Helios 2, the mean values of $\langle d_{rg} \rangle$ for RDs, TDs and EDs are quite similar compared to the radial dependence. Here, RDs are always thicker than TDs by a factor of 1.5. A similar dependence on the radial distance is observed for the thickness normalized to the ion inertial length c/ω_{pi}, where a decrease from $127\, c/\omega_{pi}$ at 0.3 AU to $2.6\, c/\omega_{pi}$ at 19 AU occurs.

Our results of radial decrease are consistent with Barnstorf (1980) between 0.3 and 1 AU. But they are not in agreement with those of Lepping and Behannon (1986), who observed no dependence between 0.46 and 1 AU.

7 Differences between discontinuities in the inner and middle heliosphere

The interval used from Voyager 2 is far away from the Sun and is located in the middle heliosphere, while the other intervals come from the inner heliosphere. In the middle heliosphere, the overall solar wind structures are changed and other processes dominate the plasma (Burlaga et al., 1977; Zank and Pauls, 1997; Whang et al., 1998). Observations of the pressure balance in the middle heliosphere indicate that the influence of the interstellar pickup ions is important (Burlaga, 1994).

In Sect. 4.1, we show the dependency of the rates of RD per day and TD per day in the different regions of the corotating interaction regions. Between 1 and 10 AU, these structures are decayed by a nonlinear and irreversible process, and a merged corotating interaction region arises (Burlaga, 1995), where the dynamic properties of the solar wind are quite different. Therefore, it is not astonishing to see that some of the properties for Voyager 2 are different. For ex-

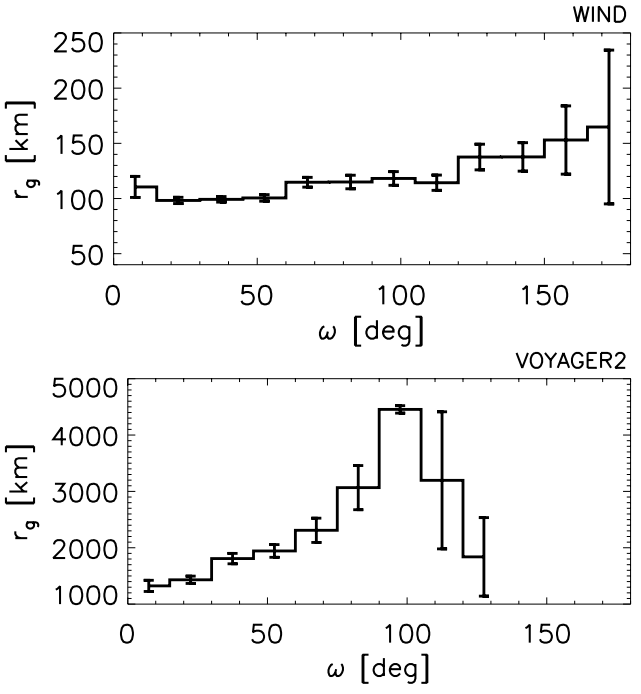

Fig. 17. Distribution of the mean r_g over the DD over ω for Wind (top) and Voyager 2 (bottom); mean error is given by the error bars.

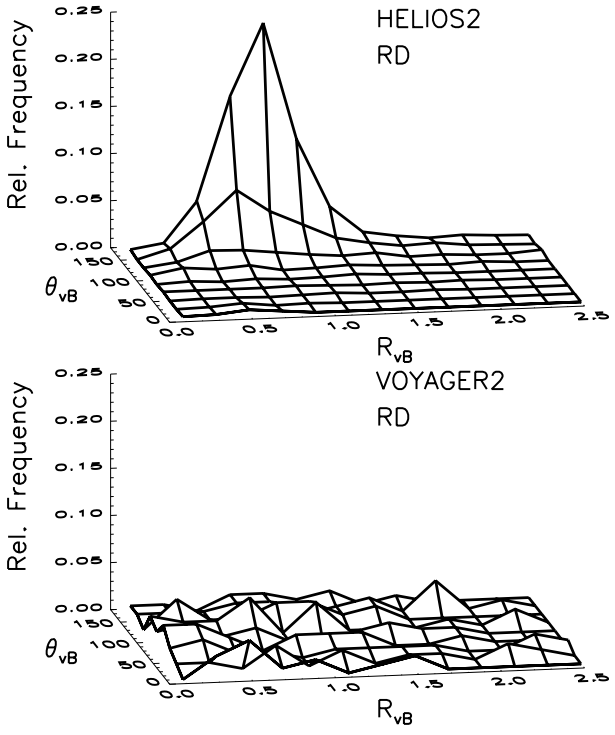

Fig. 18. Distribution of the RDs over θ_{vB} and R_{vB} for Helios 2 (top) and Voyager 2 (bottom) as a 2D histogram.

ample, the portions of the DD types are more uniformly distributed compared to the inner heliosphere (Fig. 9).

In Fig. 16, the angle γ between the normal $\boldsymbol{n}$ and the average magnetic field $\boldsymbol{B}_0$ in the transition is displayed for Ulysses II and Voyager 2. In the inner heliosphere (left plot), the orientation of the normals $\boldsymbol{n}$ depends on the orientation of the local magnetic field. For TDs, $\boldsymbol{n}$ is approximately perpendicular to $\boldsymbol{B}_0$ ($\gamma \approx 90°$) and separates different flux tubes. For RDs, $\boldsymbol{n}$ is primarily parallel to $\boldsymbol{B}_0$ ($\gamma \approx 0°$), which agrees with Alfvén waves propagating parallel to $\boldsymbol{B}_0$, but also some RDs propagating oblique to $\boldsymbol{B}_0$ exist. The orientation of $\boldsymbol{n}$ roughly depends on the Parker spiral, as previously observed by Burlaga et al. (1977), Barnstorf (1980) and Lepping and Behannon (1986). In the middle heliosphere, the distribution of γ is nearly uniform, except for the direction $\boldsymbol{n}$ parallel to $\boldsymbol{B}_0$ ($\gamma \approx 0°$). Only very few RDs propagate parallel to $\boldsymbol{B}_0$.

Another difference between the inner and the middle heliosphere is shown in Fig. 17. In the inner heliosphere (top, Wind), on average, a larger proton gyro radius r_g is connected to a larger directional change ω in the magnetic field. The increase is weak and the same interrelation is seen for the different DD types. At least for TDs, this dependence is confirmed by kinetic simulations (de Keyser et al., 1997). In the middle heliosphere (bottom), the largest r_g is connected to $\omega \approx 90°$ and the same interrelation is seen for the different DD types. The distribution decrease is much stronger for smaller and larger ω, respectively, and r_g changes by a factor of 4.

In MHD theory, RDs must fulfill the following equations:

$$[\boldsymbol{v}] = \pm \left(\frac{\rho A}{\mu_0}\right)^{1/2} \left[\frac{\boldsymbol{B}}{\rho}\right] \quad (1)$$

$$R_{vB} = \left(\frac{\mu_0}{\rho A}\right)^{1/2} \cdot \frac{|[\boldsymbol{v}]|}{|[\boldsymbol{B}/\rho]|} = 1\,. \quad (2)$$

Equation (1) indicates that $[\boldsymbol{v}]$ must be parallel or antiparallel to $[\boldsymbol{B}/\rho]$ (Alfvén relation). This means that the angle θ_{vB} between $[\boldsymbol{v}]$ and $[\boldsymbol{B}/\rho]$ must be 0° or 180°. Equation (2) results from the equipartition of the change in the mass flux and in the magnetic field in the energy density.

A 2D histogram for RDs versus θ_{vB} and R_{vB} is displayed in Fig. 18 for Helios 2 and Voyager 2. In the inner heliosphere (top, Helios 2), for most of the RDs, θ_{vB} is 180°, indicating a propagation direction away from the Sun (the sign of $\boldsymbol{B}$ is considered) and for most RDs, $R_{vB} \leq 1$. The expectation due to the Alfvénic character for Helios 2 is clearly fulfilled. In general, in the high speed solar wind, the peak is stronger than in the low speed wind.

With increasing distance from the Sun, the peak decreases and moves to smaller R_{vB} (not shown). This means that the Alfvénic character of the RDs decreases with increasing solar distance. In the middle heliosphere (bottom, Voyager 2), far away from the Sun, no peak is observed and no θ_{vb} or R_{vB} stands out. Therefore, with respect to θ_{vb} and R_{vB}, no Alfvénic character is observed. One reason why no favored θ_{vb} exists could be due to the small value of $|[\boldsymbol{v}]|$ which produces a larger error and this may be the main reason for the decreasing Alfvénic character.

8 Summary of observations and discussion

We have investigated directional discontinuities in the solar wind for 7 intervals during solar activity minimum from 5 missions with respect to the radial and latitudinal dependence in the range 0.3 to 19 AU and $+10°$ to $-80°$. The DDs are identified by the criteria of Burlaga (1969) and Tsurutani and Smith (1979).

8.1 DD types and their dependences

In the inner heliosphere, the portion of the different DD types shows no radial or latitudinal dependence. There exists approximately 55% clear RDs, 33% EDs and 10% clear TDs, with the remaining DDs as NDs. If one uses only magnetic field data, the portion of the clear TDs seems only to be a lower limit, since some of the NDs and most of the EDs are probably also TDs. Therefore, the portion of RDs is not 5 times larger than that of the TDs, but only around 1.3 times larger. If one uses the averages of the relative frequencies of the directional change ω for RDs, TDs and EDs, then the ratio RD:TD in the part of the EDs is estimated to 0.42.

But if one also uses plasma data to determine the changes of the adiabatic invariants ($T_\perp/B$, $T_\parallel B^2/n^2$) over the transition, and the ratio R_{vB} and the angle θ_{vB} for the different DD types, then many EDs display the characteristics of RDs, which has also been previously seen by Neugebauer et al. (1984). The averages of adiabatic invariants are the same for RDs and EDs. From R_{vB}, one could estimate the ratio RD:TD in the part of the EDs to be 1.7 and from θ_{vB}, to be 5.1. Therefore, it is not possible to associate the EDs clearly with RDs or TDs.

Variations in the ratios RD:TD occur at least in the order of $\pm 5\%$, as Neugebauer et al. (1984) show for intervals following each other. This indicates that longer period variations must exist. The existence of long period variations of the overall rates are observed by Tsurutani and Smith (1979) after averaging over one solar rotation.

The portions of the different DD types depend on the identification criterion used. With the TS criterion up to 10% more RDs are observed compared to the B criterion. At first glance, this is not expected because by using the TS criterion, in comparison to the B criterion, changes of magnitude are allowed, which implies favoring the identification of TDs over RDs. But magnitude changes could also lead to EDs or anisotropic RDs, which is more probably, since large magnitude changes are much more rare than directional ones (Burlaga, 1969). Due to the increasing number of DDs with small ω, it is obvious that a large number of DDs exists with ω only insignificantly smaller than 30°, where only a small change of magnitude is necessary to fulfill the TS criterion. Therefore, with the TS criterion, additional (weak) anisotropic RDs with primarily small ω (which propagate often with a large angle to the ambient magnetic field), as well as a few clear TDs are identified.

The ratio of the rates of RDs and TDs depends on the local solar wind structure. In the high speed solar wind (peak region, leading edge), the ratio is increased compared to the slow solar wind (trailing edge), due to a larger portion of RDs. This is consistent with the increased ratio in fields connected with coronal holes (open field lines) compared to regions with closed field lines. It is also consistent with a decreased ratio in subsets of CME flows that have a high helium abundance (Neugebauer and Alexander, 1991).

Though Fig. 9 may indicate a radial variation of the ratio RD/TD in view of earlier results (Barnstorf, 1980) with variability from solar rotation to solar rotation, it may be concluded that in the inner heliosphere, no clear dependence on latitude or radial distance exists on a global scale.

In the middle heliosphere, the proportions of the DD types are much more uniform and are nearly independent of the identification criteria; there are 40% RDs, 26% TDs, 14% EDs and 20% NDs. Since high speed streams are destroyed in the middle heliosphere, no variations of the ratio RD/TD, due to different solar wind velocities, could be investigated.

8.2 Evolution of ω

The distributions of the directional changes ω steepen with distance from the Sun. Fewer events with $\omega > 60°$ are observed. Therefore, the fit parameter ω_s decreases with increasing r from 82° to 50°. This indicates that the DDs appear to evolve during their lifetime in the solar wind. Whether this results in an annihilation of DDs or not, is not clear. To clarify this, a mechanism is needed which could lead to this evolution.

A change of ω during the convection of a DD in the solar wind is not surprising. Under the assumption of a parker spiral for the magnetic field, the radial evolutions of the radial and the azimuthal components differ, and therefore, the magnetic field on each side of the transition evolves differently.

For TDs, we have $\langle\omega\rangle \approx 78°$, where no ω stands out from the others and no radial dependence of the distribution inside 2.3 AU is observed. For RDs, small ω is more probable and with increasing r, fewer RDs with very large ω are observed.

A radial decrease of ω_s is seen for DDs that are identified using the TS criterion, but a clear radial constancy is observed for them for the B criterion. This indicates that the evolution of ω_s is due to the additionally identified DDs by the TS criterion, i.e. by anisotropic RDs. Since RDs are involved in the evolution, one could assume that the evolution of nonlinear steepened Alfvénic waves is connected to it, since RDs are often observed in connection with nonlinear Alfvénic waves (Tsurutani et al., 1994, 1995, 1996).

To find a mechanism for the evolution, one should look at the stability of RDs. One-dimensional hybrid simulations do not lead to definite results. While Richter and Scholer (1989) observed that RDs with $\theta_{Bn} < 45°$ are unstable, where θ_{Bn} is the angle between the upstream magnetic field and $\boldsymbol{n}$, Goodrich and Cargill (1991) observed stable RDs with $\theta_{Bn} = 30°$.

In the inner heliosphere, ω increases slightly with the proton gyro radius r_g, which may be forced by the generation mechanism. But an instability or evolution could not be ex-

cluded, because Voyager 2 DDs with $\omega \approx 90°$ have the largest r_g.

8.3 Thickness of the transition

A reason for the increase in the thickness d_{km} of DDs in the solar wind with r could be the increase of the fundamental plasma scales, for instance, the proton gyro radius r_g or the ion inertial length c/ω_{pi} (Tsurutani and Smith, 1979). The influence of the systematic error due to different time resolutions is negligible after normalization to r_g. A strong decrease in the mean d_{rg} with r occurs for all DDs by a factor of 50, as well as for each DD type itself. The same dependence is observed in the case of normalization to the ion inertial length.

Different models are developed to investigate the thickness of DDs. Sestero (1964) and Lemaire and Burlaga (1976) developed a kinetic theory for a current sheet with a smoothly varying magnetic field, especially for contact and tangential discontinuities. They predicted a thickness on the order of a few to several proton gyro radii, depending on the conditions on both sides of the current sheet. The same thickness is found in the simulation of TDs (Cargill, 1990). For RDs, the results of a hybrid simulation show that a minimum with a few ion inertial lengths exists (Krauss-Varban, 1993). At least within 2.3 AU, the observed thickness of the TDs and RDs is larger than predicted by these models. But Cargill (1990) found from hybrid simulations that the change in the magnetic field of TDs can be stretched over many proton gyro radii when a density gradient and plasma flows of the order of the Alfvén speed are present. At least in the ecliptic plane, many TDs have a density gradient.

In the case of a constant d_{rg} versus r, the current sheet is quasi-stationary and would be produced by a constant proton drift current (Lepping and Behannon, 1986). The radial dependence of d_{rg} indicates an evolution of DDs which is a strong one due to the reduction, by a factor 50, between 0.3 and 19 AU. Again, it is not clear whether an annihilation of DDs occurs or not.

8.4 Discontinuities in the middle heliosphere

Concerning the thickness, the directional change ω, the radial occurrence, as well as the velocity and latitudinal dependence of the rates, the results of the DDs of Voyager 2 (middle heliosphere) are similar to the results of the inner heliosphere. However, other properties differ.

In the middle heliosphere, the portions of the DD types are much more uniformly distributed. The orientation of the normals $\boldsymbol{n}$ are not related to the orientation of the parker spiral, although the parker model describes well the orientation of the magnetic field during the inactive period of the Sun (Burlaga, 1995). The orientation with respect to the local magnetic field is uniform, with the exception of the case where the direction of $\boldsymbol{n}$ is parallel to $\boldsymbol{B}_0$ where no DDs occur. This could indicate that RDs propagating parallel to $\boldsymbol{B}$ are unstable. But an instability must operate on a large time- or spatial-scale, since in the inner heliosphere, between 0.3 and 2.3 AU, no influence is observed. The trigger of the instability could be the temporal behavior, the change of the magnetic field or the proton gyro radius with increasing distance from the Sun, or the influence of pickup ions. Simulation studies could be helpful to discriminate among these. Also, it is not understood why DDs with $\omega \approx 90°$ are connected with a much larger proton gyro radius compared to smaller and larger ω. The average r_g varies by a factor 4 for different ω.

The Alfvénic character of DDs with respect to θ_{vB} and R_{vB} decreases with r. For Voyager 2, in most cases, $[\boldsymbol{v}]$ is not parallel to $[\boldsymbol{B}/\rho]$. This could be due to the larger error in the direction of $[\boldsymbol{v}]$ if v is small. The fact that this is not the only reason for producing this decrease is seen from the calculation of the correlation coefficients between $\boldsymbol{v}$ and $\boldsymbol{B}$ for RDs. They do not depend on the magnitude of $\boldsymbol{v}$. The portion of DDs in the ecliptic plane clearly propagating away from the Sun decreases from 63% at 1.3 AU to 29% at 19 AU. On the other hand, the portion of DDs clearly propagating towards the Sun increases from 13% at 1.3 AU to 22% at 19 AU. For the other DDs different signs of the correlation coefficients between $\boldsymbol{v}$ and $\boldsymbol{B}$ are observed. This decrease in the portion propagating away from the Sun is consistent with results from a MHD turbulence model, where the Alfvénic correlation will be destroyed due to the increased number of generated non-Alfvénic waves (Marsch and Tu, 1990).

As a final point for the comparison of the results of the inner and middle heliosphere, we should note that the interval of Voyager 2 is from a different part of the 22-year solar activity cycle, where the field orientation is reversed from that of the other intervals studied here. In addition, it takes place during the minimum of activity. However, it is unlikely that this is the reason for these regional differences.

8.5 Dependences of the rate of occurrence of DDs

The rate of occurrence of DDs depends on the radial distance from the Sun and on the solar wind velocity. These effects are independent of each other. The velocity dependence is a geometric effect. The rates increase linearly with v_{sw} if the solar wind speed is higher due to the larger investigated plasma volume. The slope of the increase varies by selection of the identification criteria. For the TS criterion, for each 100 km/s, the rate increases by about 17 DDs and for the B criterion, by about 10 DDs.

One might see a contradiction between these results and the observation that magnetic clouds essentially have no discontinuities. The intervals of Helios 2, Wind and Imp 8 each include one magnetic cloud (each around 12 h). However, their frequency of occurence is very low and thus, covers only a small fraction of time. Thus, their contribution to statistical results of this type is negligible.

With increasing distance r, the rate of occurrence decreases with $r^{-1.28}$ for the B and with $r^{-0.78}$ for the TS criterion. Three mechanisms might occur. First, all DDs are generated within 0.3 AU, and the number decreases with r. Second, the

ratio of generated to annihilated DDs increases with r. And third, the DDs will not be identified by the criteria due to changes in their temporal thickness or in their direction. A geometric effect in the velocity could not cause this decrease, if we assume that DDs are infinitely extended 1D structures. In this case, only the number of investigated volume elements is important, not the size of them.

First, we discuss the non-identification of DDs by the criteria. Due to the evolution of ω for the TS criterion, many DDs will not be identified by this criterion, since ω is too small (assuming that the magnitude of B does not greatly change). But this does not fit for the B criterion, and therefore, it could not be the main reason for the decrease in the rates. Also, the increase in the thickness (ΔT_t or d_{km}) could lead to a non-identification, if the ΔT_t is compared to the time interval used in the criteria. But since ΔT_t is short, especially near the Sun, where the strongest increase occurs, this could also not be the main reason. The evolution in d_{rg} does not lead to a non-identification, but in the case of annihilation of DDs, the rates are reduced. Therefore, the radial increase is not primarily produced by the change in the properties of DDs, which lead to a non-identification by the criteria.

However, we believe that the decrease in the rate of occurrence is not obviously due to the non-identification. The DDs are perhaps unstable (maybe as a result of the annihilation due to the evolution in ω and r_{rg}), are perhaps destroyed by any resistivity in the plasma or a spatial effect occurs which produces the gradient (Lepping and Behannon, 1986). However, the picture of DDs as curved surfaces of large dimensions may not be correct. Rather, the current sheets could have a relatively small scale. To investigate this, multi spacecraft measurements are necessary. This idea is supported by investigations of DDs with different 1D-MVA methods, which show that DDs are primarily not clearly one-dimensional, but rather two- or three-dimensional.

8.6 Variations in the rate of DD** per day

After the normalization of the rates of all DD per day to 400 km/s and 1 AU, no dependency on the heliographic latitude nor on the different solar wind structures exists. In this case, 52.3 DD** per day with the TS criterion, 17.9 DD per day with the B criterion, and 63.6 DD** per day altogether are observed. This indicates that the DDs are uniformly distributed on a sphere with constant r ($0.3 \leq r \leq 19$ AU). This does not indicate that the DDs are uniformly generated at the Sun, because the ratio of the cross section area of a flux tube at the Sun and at 0.3 AU, for example, depends on the solar wind velocity. For flux tubes connected to a coronal hole, the ratio is smaller than for flux tubes from the active region of the Sun. We investigated only the southern hemisphere, but no difference in the rate of occurrence is observable for the northern hemisphere (Tsurutani et al., 1996).

The rates of DD** per day vary markedly from day-to-day, and other influences must exist. For example, long period variations occur on the rates of DD per day averaged over one solar rotation (Tsurutani and Smith, 1979). We can only speculate if variations of solar activity influence the rate. Lepping and Behannon (1986) observed in Mariner 10 data during the decreasing phase of solar activity (November 1973 – April 1974) the same radial dependence as the study. Therefore, we expect that perhaps the absolute number of DDs varies, but not the qualitative dependences. Due to these variations, with the knowledge of the radial and velocity dependence, it is not possible to determine the solar wind velocity from the measured rate of DD per day.

8.7 Generation and annihilation of DDs

The ratio RD/TD shows a dependence on different solar wind structures which will be supported by other observations. At high heliographic latitudes, the solar wind is characterized by the presence of many large-amplitude Alfvén waves (Tsurutani et al., 1994; Goldstein et al., 1995; Smith et al., 1995). They are nonlinear and steepened. The fast rotational part of the Alfvén wave often appears in Ulysses data as a RD (Tsurutani et al., 1994, 1995, 1996). This is a plausible reason why more RDs are observed in the solar wind originating in coronal holes. The number of TDs vary much less with the solar structures.

This is consistent with the theory of Parker (1991) that the generation of TDs lead to a heating of the corona in regions with closed field lines, and that in coronal holes with open field lines, MHD waves (primarily nonlinear Alfvén waves) are important for solar wind acceleration.

The motion of the footpoints of the magnetic field lines in coronal holes with open field lines produces less winding and inwoven flux tubes than in regions with closed field lines. Therefore, in coronal holes fewer TDs are formed. Another mechanism for the generation of TDs could be microstreams, which are frequently observed at high latitudes (Neugebauer et al., 1995; McComas et al., 1995). In addition, two different types of TDs are observed (Ho et al., 1995, 1996; Tsurutani et al., 1996). One has small directional changes and is associated with the mirror mode instability, and the other one has larger directional changes and occurs at the interface between two streams. The latter type is consistent with the TDs of the Parker theory but contrasts with the former type, which is locally generated.

RDs propagate primarily away from the Sun. The ratio of the outward to inward propagating RDs is higher than the analogous ratio for Alfvén waves (Neugebauer and Buti, 1990). This indicates that Alfvén waves propagating inward are less steepened, caused perhaps by the smaller amplitude of local generated waves.

However, different generation mechanisms for RDs and TDs have been shown, which primarily produce DDs at or near the Sun. These mechanisms have no influence on the radial dependence of the rates. The portion of locally generated DDs is small (maybe negligible). The question of whether their generation mechanism depends on radial distance is not investigated here.

Different annihilation mechanisms are discussed. Neuge-

bauer et al. (1986) suggest that the Kelvin-Helmholtz instability may destroy TDs. For this mechanism, stability depends on the orientation of $\boldsymbol{B}$ relative to $[\boldsymbol{v}]$ (Sen, 1963). A parallel case stabilizes the discontinuity. With the assumption of large directional changes, the stability is also valid for $[\boldsymbol{B}]$ (Neugebauer et al., 1984). DDs with large $[\boldsymbol{v}]$ which are not parallel to $[\boldsymbol{B}/\rho]$ are unstable. This could be a reason why TDs show an Alfvénic character. Due to the growth of the Kelvin-Helmholtz instability with decreasing Alfvén velocity (Neugebauer et al., 1984), this could lead to a radial distance dependence.

Connected with the generation and annihilation of DDs, the question arises about the generation of DDs: are they triggered by any mechanism? But for all investigated intervals, the distribution of the inter-arrival time is Poisson-distributed. This indicates that each DD is statistically independently generated which is inconsistent with a process of triggering.

Acknowledgement. We thank Max Schroeder for his help by the visual inspection of the discontinuities and Katja Sperveslage for helpful discussion. We thank the principal investigators of the Helios 2, WIND, IMP 8, Ulysses and Voyager 2 magnetometer and plasma instruments for using their data and the data processing teams for their efforts. The work by A. S. and F. M. N. was supported financially by DARA/DLR.

Topical Editor E. Antonucci thanks a referee for his help in evaluating this paper.

References

Bame, S. J., McComas, D. J., Barraclough, B. L., Phillips, J. L., Sofaly, K. J., Chavez, J. C., Goldstein, B. E., and Sakurai, R. K., The Ulysses solar wind plasma experiment, Astron. Astrophys. Suppl. Ser., 92, 237–265, 1992.

Barnstorf, H., Stromschichten im interplanetaren Raum, Dissertation, TU Braunschweig, 1980.

Behannon, K. W., Acuña, M. H., Burlaga, L. F., Lepping, R. P., Ness, N. F., and Neubauer, F. M., Magnetic field experiment for Voyagers 1 and 2, Space Sci. Rev., 21, 235–257, 1977.

Belcher, J. W. and Solodyna, C. V., Alfvén waves and directional discontinuities in the interplanetary medium, J. Geophys. Res., 80(1), 181, 1975.

Burlaga, L. F., Directional discontinuities in the interplanetary magnetic field, Sol. Physics, 7, 54, 1969.

Burlaga, L. F., Hydromagnetic waves and discontinuities in the solar wind, Space Sci. Rev., 12, 600–657, 1971a.

Burlaga, L. F., On the nature and origin of directional discontinuities in the solar wind, J. Geophys. Res., 76(19), 4360, 1971b.

Burlaga, L. F., Shocks in the outer heliosphere: Voyager 2 observations from 18.9 AU to 30.2 AU (1986–1989), J. Geophys. Res., 99(A3), 4161–4171, 1994.

Burlaga, L. F., Interplanetary Magnetohydrodynamics, Oxford Univ. Press, 1995.

Burlaga, L. F., Lemaire, J. F., and Turner, J. M., Interplanetary current sheets at 1 AU, J. Geophys. Res., 82(22), 3191–3200, 1977.

Cargill, P. J., Hybrid simulations of tangential discontinuities, Geophys. Res. Lett., 17(8), 1037–1040, 1990.

de Keyser, J., Roth, M., Tsurutani, B. T., Ho, C. M., and Phillips, J. L., Solar wind velocity jumps across tangential discontinuities: Ulysses observations and kinetic interpretation, Astron. Astrophys., 321, 945–959, 1997.

Goldstein, B. E., Neugebauer, M., and Smith, E. J., Alfvén waves, alpha particles, and pickup ions in the solar wind, Geophys. Res. Lett., 22(23), 3389–3392, 1995.

Goodrich, C. C. and Cargill, P. J., An investigation of the structure of rotational discontinuities, Geophys. Res. Lett., 18(1), 65–68, 1991.

Hartle, R. E., Sittler, E. C., Ogilvie, K. W., Scudder, J. D., Lazarus, A. J., and Atreya, S. K., Titan's ion exosphere observed from Voyager 1, J. Geophys. Res., 87(A3), 1383–1394, 1982.

Ho, C. M., Tsurutani, B. T., Goldstein, B. E., Phillips, J. L., and Balogh, A., Tangential discontinuities at high heliographic latitudes ($\sim -80°$), Geophys. Res. Lett., 22, 3409, 1995.

Ho, C. M., Tsurutani, B. T., Sakurai, R., Goldstein, B. E., Balogh, A., and Phillips, J. L., Interplanetary discontinuities in corotating streams and their interaction regions, Astron. Astrophys., 316, 346–349, 1996.

Krauss-Varban, D., Structure and length scales of rotational discontinuities, J. Geophys. Res., 98(A3), 3907–3917, 1993.

Lemaire, J. and Burlaga, L. F., Diamagnetic boundary layers: A kinetic theory, Astrophys. Space Sci., 45, 303–325, 1976.

Lepping, R. P. et al., The WIND magnetic field investigation, Space Sci. Rev., 71, 207–229, 1995.

Lepping, R. P. and Behannon, K. W., Magnetic field directional discontinuities: Characteristics between 0.46 and 1.0 AU, J. Geophys. Res., 91, 8725, 1986.

Mariani, F., Bavassano, B., Villante, U., and Ness, N. F., Variations of the occurence rate of discontinuities in the interplanetary magnetic field, J. Geophys. Res., 78(34), 8011, 1973.

Marsch, E. and Tu, C.-Y., On the radial evolution of MHD turbulence in the inner heliosphere, J. Geophys. Res., 95(A6), 8211–8229, 1990.

McComas, D. J., Barraclough, B. L., Gosling, J. T., Hammond, C. M., Phillips, J. L., Neugebauer, M., Balogh, A., and Forsyth, R. J., Structures in the polar solar wind: Plasma and field observation from Ulysses, J. Geophys. Res., 100(A10), 19893–19902, 1995.

Musmann, G., Neubauer, F. M., and Lammers, E., Radial variation of the interplanetary magnetic field between 0.3 AU and 1.0 AU: Observations by the Helios-1 spacecraft, J. Geophys. Res., 42, 591–598, 1977.

Neugebauer, M. and Alexander, C. J., Shuffling foot points and magnetohydrodynamic discontinuities in the solar wind, J. Geophys. Res., 96(A6), 9409–9418, 1991.

Neugebauer, M., Alexander, C. J., Schwenn, R., and Richter, A. K., Tangential discontinuities in the solar wind: Correlated field and velocity changes and the Kelvin-Helmholtz instability, J. Geophys. Res., 91(A12), 13694–13698, 1986.

Neugebauer, M. and Buti, B., A search for evidence of the evolution of rotational discontinuities in the solar wind from nonlinear Alfvén waves, J. Geophys. Res., 95(A1), 13–20, 1990.

Neugebauer, M., Clay, D. R., Goldstein, B. E., Tsurutani, B. T., and Zwickl, R. D., A reexamination of rotational and tangential discontinuities in the solar wind, J. Geophys. Res., 89(A7), 5393–5408, 1984.

Neugebauer, M., Goldstein, B. E., McComas, D. J., Suess, S. T., and Balogh, A., Ulysses observations of microstreams in the solar wind from coronal holes, J. Geophys. Res., 100(A12), 23389–23395, 1995.

Parker, E. N., Space plasma and its origin at the sun, Phys. Fluids B, 3(8), 2367–2373, 1991.

Richter, P. and Scholer, M., On the stability of rotational discontinuities, Geophys. Res. Lett., 16(11), 1257–1260, 1989.

Rosenbauer, H., Schwenn, R., Marsch, E., Meyer, B., Miggenrieder, H., Montgomery, M. D., Mühlhäuser, K.-H., Pilipp, W., Voges, W., and Zink, S. M., A survey on initial results of the Helios plasma experiment, J. Geophys., 42(6), 561–580, 1977.

Sen, A. K., Stability of hydromagnetic Kelvin-Helmholtz discontinuity, Phys. Fluids, 6(8), 1154–1163, 1963.

Sestero, A., Structure of plasma sheaths, Phys. Fluids, 7(1), 44–51, 1964.

Smith, E. J., Identification of interplanetary tangential and rotational discontinuities, J. Geophys. Res., 78, 2054, 1973.

Smith, E. J., Balogh, A., Neugebauer, M., and McComas, D., Ulysses observations of Alfvén waves in the southern and northern solar hemispheres, Geophys. Res. Lett., 22(23), 3381–3384, 1995.

Solodyna, C. V., Sari, J. W., and Belcher, J. W., Plasma field characteristics of directional discontinuities in the interplanetary medium, J. Geophys. Res., 82(1), 10, 1977.

Sonnerup, B. U. Ö. and Cahill, L. J., Magnetopause structure and attitude from Explorer 12 observations, J. Geophys. Res., 72(A1), 171–183, 1967.

Tsurutani, B. T., Glaßmeier, K.-H., and Neubauer, F. M., An intercomparision of plasma turbulence at three comets: Grigg-Skjellerup, Giacobini-Zinner, and Halley, Geophys. Res. Lett., 22(9), 1149–1152, 1995.

Tsurutani, B. T., Ho, C. M., Arballo, J. K., Smith, E. J., and Goldstein, B. E., Interplanetary discontinuities and Alfvén waves at high heliographic latitudes: Ulysses, J. Geophys. Res., 101(A5), 11027–11038, 1996.

Tsurutani, B. T., Ho, C. M., Sakurai, R., Goldstein, B. E., Balogh, A., and Phillips, J. L., Symmetry in discontinuity properties at the north and south heliographic poles: Ulysses, Astron. Astrophys., 316, 342–345, 1996.

Tsurutani, B. T., Ho, C. M., Smith, E. J., Neugebauer, M., Goldstein, B. E., Mok, J. S., Arballo, J. K., Balogh, A., Southwood, D. J., and Feldmann, W. C., The relationship between interplanetary discontinuities and Alfvén waves: Ulysses observations, Geophys. Res. Lett., 21, 2267–2270, 1994.

Tsurutani, B. T. and Smith, E. J., Interplanetary discontinuities: Temporal variations and the radial gradient from 1 to 8 AU, J. Geophys. Res., 84, 2773, 1979.

Whang, Y. C., Zhou, J., Lepping, R. P., Szabo, A., Fairfield, D., Kokubun, S., Ogilvie, K. W., and Fitzenreiter, R. J., Double discontinuity: A compound structure of slow shock and rotational discontinuity, J. Geophys. Res., 103(A4), 6513–6520, 1998.

Zank, G. P. and Pauls, H. L., Shock propagation in the outer heliosphere; 1. pickup ions and gasdynamics, J. Geophys. Res., 102(A4), 7037–7049, 1997.